

AD A032699

AFGL-TR-76-0238

RESEARCH IN SEISMOLOGY: EARTHQUAKE MAGNITUDES

Otto W. Nuttli  
So Gu Kim  
Huei-Yuin Wen  
John A. Wagner

Department of Earth and Atmospheric Sciences  
Saint Louis University  
St. Louis, Missouri 63103

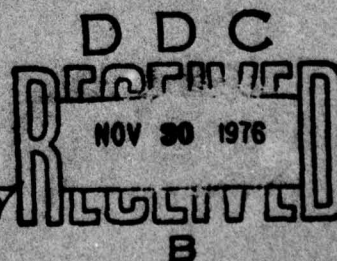
11 October 1976

Final Report  
1 July 1973 - 30 September 1976

Approved for public release; distribution unlimited.

This research was sponsored by the Defense Advanced  
Research Projects Agency. ARPA Order No. 1795

AIR FORCE GEOPHYSICS LABORATORY  
AIR FORCE SYSTEMS COMMAND  
UNITED STATES AIR FORCE  
HANSCOM AFB, MASSACHUSETTS 01731





ARPA Order No. 1795  
Program Code No. 3F10  
Contractor: Saint Louis University  
Effective Date of Contract:  
1 July 1973

Contract No. F19628-73-C-0269  
Principal Investigator & Phone No.:  
Otto W. Nuttli/314-535-3300,  
Ext. 547B

AFGL Project Scientist:  
Lieutenant Mark Settle  
Contract Expiration Date:  
30 September 1976.

Qualified requestors may obtain additional copies from the  
Defense Documentation Center. All others should apply to the  
National Technical Information Service.

Unclassified

SECURITY CLASSIFICATION OF THIS PAGE (When Data Entered)

REPORT DOCUMENTATION PAGE		READ INSTRUCTIONS BEFORE COMPLETING FORM
1. REPORT NUMBER AFGL-TR-76-0238	2. GOVT ACCESSION NO.	3. RECIPIENT'S CATALOG NUMBER
4. TITLE (and Subtitle) RESEARCH IN SEISMOLOGY: EARTHQUAKE MAGNITUDES.	5. TYPE OF REPORT & PERIOD COVERED Final Report. 1 Jul 1973-30 Sep 1976	6. PERFORMING ORG. REPORT NUMBER
7. AUTHOR(s) Otto W. Nuttli, So Gu/Kim, Huei-Yuin/Wen John A. Wagner	8. CONTRACT OR GRANT NUMBER(s) F19628-73-C-0269 ARPA Order-1795	9. PROGRAM ELEMENT, PROJECT, TASK AREA & WORK UNIT NUMBERS PE 62701E-Project 1795 T, WU & SE n/a
10. PERFORMING ORGANIZATION NAME AND ADDRESS Dept. of Earth and Atmospheric Sciences Saint Louis University St. Louis, MO 63103	11. CONTROLLING OFFICE NAME AND ADDRESS Air Force Geophysics Laboratory Hanscom AFB, MA 01731 Contract Monitor: Lt. Mark Settle /LWW	12. REPORT DATE 11 October 1976
13. MONITORING AGENCY NAME & ADDRESS (if different from Controlling Office) 12/52p	14. SECURITY CLASS. (of this report) Unclassified	15. DECLASSIFICATION/DOWNGRADING SCHEDULE
16. DISTRIBUTION STATEMENT (of this Report) Approved for public release; distribution unlimited. 16/1795		
17. DISTRIBUTION STATEMENT (of the abstract entered in Block 20, if different from Report)		
18. SUPPLEMENTARY NOTES This research was sponsored by the Defense Advanced Research Projects Agency under ARPA Order No. 1795.		
19. KEY WORDS (Continue on reverse side if necessary and identify by block number) Nuclear explosions      Seismic Discrimination Earthquakes              Aftershocks Magnitudes                Eurasia <i>ratios of body-wave magnitude to surface-wave magnitude</i>		
20. ABSTRACT (Continue on reverse side if necessary and identify by block number) This report presents the results of a search for earthquakes in Eurasia that have anomalous $m_b$ - $M_s$ values, where $m_b$ is body- wave magnitude and $M_s$ is surface-wave magnitude. The report also presents the results of a study of mainshock-aftershock sequences. <i>are also provided.</i> Earthquakes occurring along the plate margin of Eurasia were found to be non-anomalous. The anomalous earthquakes are (over)		

DD FORM 1 JAN 73 1473 EDITION OF 1 NOV 65 IS OBSOLETE

Unclassified

SECURITY CLASSIFICATION OF THIS PAGE (When Data Entered)

405292

LB



Unclassified

SECURITY CLASSIFICATION OF THIS PAGE(When Data Entered)

Block 20. (cont'd) *Pr p1473A*

*(M sub b): (M sub S)*

*Continental*  
→ confined to the interior of the continent, with about 18% of the intraplate earthquakes studied having anomalous  $m_p M_g$  values; The anomalous events are not restricted to any geographic area, but extend from southern Europe to eastern Asia.

Anomalous earthquakes are often found among the aftershocks of mainshock-aftershock intraplate earthquake sequences. It

was found that the focal depth and focal mechanisms of anomalous and non-anomalous earthquakes of the sequences studied

were the same, so that depth and mechanism variations do not provide an explanation of these anomalous events. Furthermore,

*were found to be anomalies.* → it was found that the anomalous earthquakes had shorter P-wave spectral corner periods than non-anomalous earthquakes of the same surface-wave magnitude or seismic moment. Our results suggest that it would be especially difficult to discriminate between a small-magnitude aftershock of an intraplate earthquake and a small to intermediate yield explosion detonated within a few hours or days of the mainshock. *It appears to explain the*

ACCESSION for	
NTIS	White Section <input checked="" type="checkbox"/>
DOC	Buff Section <input type="checkbox"/>
UNANNOUNCED	<input type="checkbox"/>
JUSTIFICATION .....	
BY .....	
DISTRIBUTION/AVAILABILITY CODES	
Dist. AVAIL. and/or SPECIAL	
<i>A</i>	

Unclassified

SECURITY CLASSIFICATION OF THIS PAGE(When Data Entered)



## INTRODUCTION

For a long time it has been known that large underground nuclear explosions have small  $M_S$  values compared to earthquakes having the same  $m_b$  values as those of the explosions. This conclusion has been found also to be generally true for intermediate and smaller sized explosions. That is, when a plot of the  $m_b$  values as abscissae and  $M_S$  values as ordinates is made, the earthquakes separate from the explosions, with the latter lying below and to the right of the earthquake points. However, it has been found that some earthquakes plot in or near the explosion population. These are called anomalous earthquakes.

The primary purpose of this research is to search for shallow-depth Eurasian earthquakes that have anomalous  $m_b:M_S$  values. Furthermore, because it is for intermediate to small magnitude events that it is most difficult to discriminate between earthquakes and explosions, events were selected which had  $m_b$  values in the range of 4 to 5.5.

Other aims of the research are to identify geographical regions where anomalous earthquakes occur, to determine the effect, if any, of focal depth and focal mechanism on observed  $m_b:M_S$  values, to investigate differences in the P-wave spectra of anomalous and non-anomalous earthquakes, and to determine Love-wave  $M_S(M_{S,L})$  values for anomalous earthquakes.

## METHODOLOGY

Standard techniques were used for determining the  $m_b$  and  $M_S$  values of the earthquakes and explosions studied. That is, for  $m_b$  evaluation the largest amplitude in the first 3 cycles of the P-wave motion on the vertical-component, short-period seismogram was used, along with the Gutenberg-Richter (Richter, 1958) calibrating function. Average  $m_b$  values, along with their standard deviations and the number of stations used, are reported, as well as average  $m_b$  values and the number of stations as given by the National Earthquake Information Center and the International Seismological Centre.

To determine  $M_S$  the largest amplitude of the vertical component Rayleigh-wave motion in the period range of 17 to 23 seconds was used, along with the formulas

$$M_S = 3.30 + 1.66 \log \Delta + \log A/T \quad \text{for } 25^\circ \leq \Delta \leq 140^\circ$$

and

$$M_S = 4.16 + 1.07 \log \Delta + \log A/T \quad \text{for } 10^\circ \leq \Delta \leq 25^\circ$$

where  $\Delta$  is the epicentral distance in degrees,  $A$  is the maximum ground motion in microns, and  $T$  is the period in seconds. We examined the use of  $M_S$  formulas derived for waves of periods substantially less than 20 seconds as recorded at small to regional distances, and found in general that they were not as satisfactory as the second of the formulas given above (Nuttli and Kim, 1975). Mean  $M_S$  values, along with their standard deviations and number of stations used, are presented. In general the National Earthquake Information Center does not determine  $M_S$  values for small to intermediate magnitude events, and the International Seismological Centre never determines  $M_S$  values.

The seismograph stations whose data were used to determine  $m_b$  and  $M_S$  values were the World-Wide Standard Seismograph Network (WWSSN) stations ALQ, AQU, BLA, EUL, CHG, COL, JCT, DUG, GOL, KOD, KON, NIL, KBL, LPS, MAT, KES, NDI, NHA, OGD, QUE, SEO, SHI and SHL and the Very Long Period Experiment (VLPE) stations FBK, ALQ, TLO, CHG, CTA and EIL.

Focal depths were determined for a selected number of earthquakes, principally by means of the depth phases  $pP$  and  $sS$ . When depths of earthquakes in an aftershock sequence were compared, we also used the period of the minimum in the Rayleigh-wave spectrum. The latter method is principally of value in establishing that two or more earthquakes of the same region have the same depth, rather than in making an absolute determination of that depth.

#### DATA

Much of the basic  $m_b:M_S$  data have already been presented in Scientific Report No. 1 (Nuttli and Kim, 1974) and Scientific Report No. 3 (Nuttli, Kim and Wen, 1975). In Report No. 1 data for 96 earthquakes and 10 underground explosions were given, and in Report No. 3 the  $m_b:M_S$  values for 155 earthquakes and 4 explosions were presented. Inasmuch as these reports are readily available, a relisting of these data will not be given here.



Table 1 presents the hypocentral coordinates of 37 earthquakes and 9 explosions whose  $m_b:M_s$  values have not been included in any previous report. Table 2 gives the  $m_b$  and  $M_s$  values of the events described in Table 1.

The 23 nuclear explosions took place at the testing sites in Novaya Zemlya, eastern Kazakhstan and western Kazakhstan and at scattered sites in western Russia. Figure 1 is a plot of the  $m_b:M_s$  values of these explosions. The dashed line in the figure is the curve obtained by Evernden et al (1971) from Nevada Test Site data when  $M_s$  was determined from 20-second period Rayleigh waves. The two solid-line curves mark the envelopes or outer bounds of the Eurasian data. From the upper of these two curves we can see that all the explosion data satisfy the relation

$$m_b - M_s \geq 1.2 \quad \text{for } m_b \geq 4.6.$$

The single point  $m_b = 4.4$ ,  $M_s = 3.3$  of Figure 1 suggests that for  $m_b < 4.6$  the difference  $m_b - M_s$  may become smaller than 1.2, with the difference decreasing as  $m_b$  decreases. However, much more data in the small magnitude range than we have are required to justify such a conclusion.

Table 3 contains a list of 33 earthquakes, out of the 278 studied, which had  $m_b$  minus  $M_s$  values of 1.2 or greater, and which thus would overlap the explosion population on an  $m_b:M_s$  diagram. The  $m_b:M_s$  values of these earthquakes are plotted in Figure 2, along with the explosion bounds as determined from Figure 1. From Figure 2 it can be seen that the anomalous earthquakes listed in Table 3 have  $m_b:M_s$  values that spread over the range of explosion values.

Considering next the non-anomalous earthquakes, our data indicate that shallow oceanic margin earthquakes (Aleutians, Kamchatka, Japan, Taiwan, Philippines, New Hebrides, New Britain) all have  $m_b:M_s$  values to the left and above the upper-bound curve of the explosion population. Thus they present no problem in being distinguished from explosions. Figure 3 is a plot of  $m_b:M_s$  values of oceanic margin earthquakes.

All of the anomalous earthquakes that are listed in Table 3 and plotted in Figure 2 are intraplate earthquakes.

Not all intraplate earthquakes, however, are anomalous. Thus, for example, of the 128 intraplate earthquakes that we studied for the year 1972, only 23 had anomalous  $m_b:M_s$  values.

For the 1972 earthquakes, surface-wave magnitudes were calculated using Love-wave amplitudes as well as the amplitudes of the vertical-component Rayleigh waves. Of the 122 earthquakes for which Love-wave  $M_s$  values could be determined, only 19 had  $|M_{s,R} - M_{s,L}| > 0.3$ . Thus, in most cases, the  $M_{s,R}$  and  $M_{s,L}$  values were essentially the same. Of the 19 which showed a significant difference, only 6 had  $M_{s,L} > M_{s,R}$ . Thus there is little evidence of small  $M_{s,R}$  values compared to  $M_{s,L}$  values, as might be expected to occur if the focal depth were such that there would be a minimum in the Rayleigh-wave spectrum at a period near 20 seconds. From this we conclude that focal depth (unless it is very large, i.e. greater than the crustal thickness) cannot generally be called upon to explain small  $M_s$  values of earthquakes, and thus anomalous  $m_b:M_s$  values.

Evernden (1976) discussed the use of  $M_{s,L}$  values to discriminate between earthquakes and explosions. At places where the release of regional tectonic strain by the explosion is low, the resulting  $M_{s,L}$  values are small compared to the  $M_{s,R}$  values. Of the 23 explosions considered in this report, Love waves of 20-second period could be identified for only two. The first is the East Kazakhstan explosion of 16 August 1972, for which a very small amplitude Love wave was tentatively identified at a single VLPE station (KON). For this event  $M_{s,R}$  is 3.7 and  $M_{s,L}$  is 3.0. The second event occurred in Novaya Zemlya on 28 August 1972. It was a large explosion, and 20-second period Love waves were identified at 18 stations. For it  $M_{s,R}$  was 5.0 and  $M_{s,L}$  was 4.6.

#### MAINSHOCK-AFTERSHOCK SEQUENCES

One of the most important findings of this study was that some aftershocks of a sequence can have anomalous  $m_b:M_s$  values, whereas the mainshock and other aftershocks have non-anomalous values. This finding is particularly important because it enables us to obtain a better understanding of the cause of anomalous earthquakes, by eliminating as an explanation certain characteristics that are often proposed as the causes of anomalous  $m_b:M_s$  values.



Among these are the source and receiver crust and the transmission path, which are identical for all events of a sequence for a given seismograph station, and the focal depth and focal mechanism, which are shown to be the same for selected events of selected sequences.

A more complete discussion of the data and conclusions is given in Appendix 1, which is a manuscript of a paper submitted for publication. In this section of the report we merely present some of the data and summarize the conclusions.

Mainshock-aftershock sequences in Szechwan province of China, Tibet, the Iraq-Iran border region and the New Hebrides islands were investigated. Table 4 lists the hypocentral coordinates and the  $m_b$  and  $M_0$  values of the earthquakes studied. For the events which were of sufficiently large magnitude, focal mechanisms and P and Rayleigh-wave spectra were determined. The focal mechanism solutions verified that the earthquakes of a given sequence had nearly identical mechanisms, and the Rayleigh-wave spectra, along with the time differences pP-P and sS-S, established that the events of a given sequence had nearly identical focal depths.

From the P-wave spectra it was found that for earthquakes of the same  $M_0$  or seismic moment,  $M_0$ , the anomalous earthquakes had smaller spectral corner periods than the non-anomalous ones. This indicated that there is a relative enrichment of the short-period part of the spectrum for the anomalous earthquakes. Observations in the time domain showed that for earthquakes of the same  $m_b$  the duration of the short-period P-wave motion was smaller (more pulse-like) for anomalous than for non-anomalous earthquakes, even though the maximum amplitude of the P-wave motion was the same.

Although we have no conclusive explanation as to the cause of the anomalous aftershocks, the observations in both the frequency and time domains suggest they are related to the time history of the fault rupture and possibly to the stress drop.

#### RELEVANCE OF THE RESEARCH TO THE DISCRIMINATION OF UNDERGROUND EXPLOSIONS

One point of immediate significance is the finding that anomalous earthquakes do not occur at plate margins, but rather only within the Eurasian plate. (We did not

look at earthquakes in other continental areas.) Because earthquakes occurring along plate margins constitute the great majority of earthquakes, our finding suggests that for this large class of earthquakes the  $m_b:M_s$  criterion will readily separate explosions from earthquakes.

A second point of significance is that the anomalous earthquakes of Eurasia are not restricted to any single or few geographic areas. Table 3 demonstrates that they occur anywhere from southern Europe to eastern Asia.

Although from theory one might expect a minimum in the Rayleigh-wave spectrum at 20-second period for a certain range of focal depths within the crust, and thus anomalous  $m_b:M_s$  values for these earthquakes, our data suggest that for actual earthquakes recorded at a sufficient number of stations this is not an important phenomenon. Nor does the character of the fault motion, whether it be strike-slip or thrust faulting, lead to anomalous  $m_b:M_s$  values by itself if the Rayleigh waves are recorded over a sufficient range of azimuth.

The mainshock-aftershock studies indicate that for some cases, at least, it is not focal depth, focal mechanism, source crust, crust-mantle transmission path or receiver crust which is the cause of anomalous  $m_b:M_s$  values. Whatever is the explanation, it causes the P-wave spectra to be enriched at the short periods for the anomalous earthquakes by shifting the spectral corner period (or periods) to smaller values. Our finding that anomalous  $m_b:M_s$  earthquakes fairly often occur as aftershocks of intraplate earthquakes suggests that it might be a difficult task to distinguish between a small magnitude explosion and an aftershock of an intraplate earthquake, if the explosion were deliberately detonated after the mainshock.

#### REFERENCES

- Evernden, J. F. (1976). Study of seismological evasion Part I. General discussion of various evasion schemes, Bulletin of the Seismological Society of America, 66, 245-280.
- Evernden, J. F., W. J. Best, P. W. Pomeroy, T. V. McEvelly, J. M. Savino, and L. R. Sykes (1971). Discrimination between small-magnitude earthquakes and explosions, Journal of Geophysical Research, 76, 8042-8055.



Nuttli, O. W. and S. G. Kim (1974). Research in Seismology: Earthquake Magnitudes, Scientific Report No. 1, AFCRL-TR-74-0326, Air Force Cambridge Research Laboratories, Hanscom AFB, Massachusetts.

Nuttli, O. W. and S. G. Kim (1975). Surface-wave magnitudes of Eurasian earthquakes and explosions, Bulletin of the Seismological Society of America, 65, 693-709.

Nuttli, O. W., S. G. Kim, and H. Y. Wen (1975). Research in Seismology: Earthquake Magnitudes, Scientific Report No. 3, AFCRL-TR-75-0433, Air Force Cambridge Research Laboratories, Hanscom AFB, Massachusetts.

Richter, C. F. (1958). Elementary Seismology, W. H. Freeman and Company, San Francisco.

PUBLICATIONS RESULTING FROM RESEARCH  
PERFORMED UNDER CONTRACT F19628-73-C-0269

Nuttli, O. W. and S. G. Kim (1974). Research in Seismology: Earthquake Magnitudes, Scientific Report No. 1, AFCRL-TR-74-0326, Air Force Cambridge Research Laboratories, Hanscom AFB, Massachusetts.

Duda, S. J. and O. W. Nuttli (1974). Earthquake magnitude scales, Geophysical Surveys, 1, 429-458.

Nuttli, O. W., S. G. Kim and H. Y. Wen (1975). Research in Seismology: Earthquake Magnitudes, Scientific Report No. 3, AFCRL-TR-75-0433, Air Force Cambridge Research Laboratories, Hanscom AFB, Massachusetts.

Nuttli, O. W. and S. G. Kim (1975). Surface-wave magnitudes of Eurasian earthquakes and explosions, Bulletin of the Seismological Society of America, 65, 693-709.

Kim, S. G. (1976). Spectral Scaling of Earthquakes in Some Eurasian Aftershock Sequences, Doctoral Dissertation, Saint Louis University, 203 pp.

Kim, S. G. and O. W. Nuttli (1976). Spectral and magnitude characteristics of anomalous Eurasian earthquakes, submitted to the Bulletin of the Seismological Society of America.

TABLE 1. HYPOCENTRAL COORDINATES OF EVENTS STUDIED

Event No. <sup>a</sup>	Date	Origin Time <sup>b</sup>	Lat. (°N) <sup>b</sup>	Long. (°E) <sup>b</sup>	Depth (km) NEIC ISC	Location
1	03-07-72	02-10-00.4	30.1	50.8	38	Iran
2	03-07-72	21-38-22.2	30.0	51.0	43	Iran
3	05-07-72	01-09-52.9	44.6	81.1	33	N. Sinkiang
4	05-07-72	04-09-49.0	43.6	87.9	33	N. Sinkiang
5E	06-07-72	01-02-57.7	49.7	78.0	0	E. Kazakhstan
6	07-07-72	12-04-11.6	20.5	98.1	27	Burma
7E	09-07-72	06-59-57.9	49.8	35.4	0	S.W. Russia
8	10-07-72	19-03-33.0	43.4	88.6	33	N. Sinkiang
9	16-07-72	02-20-23.6	32.5	95.9	33	Tibet
10	16-07-72	03-39-59.8	32.6	95.8	33	Chinghai
11	21-07-72	16-08-12.1	22.6	121.5	21	Taiwan
12	22-07-72	05-10-39.5	44.9	36.9	33	S. W. Russia
13	22-07-72	16-41-04.0	31.4	91.5	33	Tibet
14	22-07-72	21-00-08.6	31.4	91.4	33	Tibet
15	09-08-72	19-42-17.3	53.0	107.5	33	Lake Balkal
16	10-08-72	21-06-40.1	32.4	93.5	33	Tibet
17	11-08-72	02-22-14.2	44.7	102.0	33	Mongolia
18	12-08-72	23-47-57.3	41.1	22.7	12	Yugoslavia
19E	16-08-72	03-16-57.2	49.8	78.1	0	E. Kazakhstan
20E	20-08-72	02-59-57.9	49.5	48.2	0	W. Kazakhstan
21E	26-08-72	03-46-56.9	50.0	77.8	0	E. Kazakhstan
22E	28-08-72	05-59-56.5	73.3	55.1	0	Novaya Zemlya
23	30-08-72	15-14-09.9	36.7	96.5	17	Chinghai
24	31-08-72	14-03-16.3	52.3	95.4	21	Central Russia
25E	02-09-72	08-56-57.6	50.0	77.7	0	E. Kazakhstan
26	02-09-72	10-37-39.4	39.9	53.7	33	Turkmenia
27	03-09-72	17-46-17.2	36.0	73.3	33	N. W. Kashmir
28	03-09-72	20-32-18.4	35.9	73.5	49	N. W. Kashmir
29E	14-09-72	07-00-03.6	67.7	33.4	7	W. Russia



TABLE 1. (Continued)

30	10-09-72	20-57-57.1	39.2	81.3	33	38	S. Sinkiang
31E	21-09-72	09-00-01.2	52.1	52.0	28	28	W. Russia
32	27-09-72	00-08-29.9	30.3	101.7	33	0	Szechwan
33	27-09-72	02-03-39.1	33.9	72.7	46	41	Pakistan
34	29-09-72	13-56-59.5	39.7	77.8	33	36	S. Sinkiang
35	29-09-72	16-21-38.0	30.4	101.5	33	3	Szechwan
36	29-09-72	20-24-42.0	30.3	101.7	33	33	Szechwan

a An "E" indicates a presumed underground nuclear explosion.

b The values given were determined by the National Earthquake Information Center (NEIC), Boulder, Colorado.

TABLE 2. BODY-WAVE ( $m_b$ ) AND SURFACE-WAVE ( $M_S$ ) MAGNITUDES OF EVENTS STUDIED.

Event No.	$m_b$ (NEIC) <sup>b</sup>	$m_b$ (ISC) <sup>b</sup>	$m_b$ <sup>b,c</sup>	$M_S$ (NEIC) <sup>b</sup>	$M_S$ , RZ <sup>b,c</sup>	$M_S$ , L <sup>b,c</sup>
1	5.0(8)	4.9(20)	4.79±0.18(5)	---	4.06±0.41(18)	3.99±0.26(b)
2	5.1(7)	4.9(23)	4.85±0.19(5)	---	4.66±0.65(23)	4.60±0.40(4)
3	4.6(2)	4.2(4)	4.01±0.40(2)	---	4.08±0.35(23)	4.24±0.40(8)
4	4.3(3)	4.2(4)	4.02±0.17(2)	---	3.31±0.34(5)	---
5	4.4(4)	4.4(6)	---	---	3.35±0.01(3)	---
6	5.0(7)	4.8(21)	5.17±0.39(9)	5.5(2)	5.04±0.30(25)	5.30±0.31(12)
7	---	4.8(5)	4.33±0.47(6)	---	3.43±0.33(5)	---
8	4.7(2)	4.5(4)	3.50(1)	---	3.87±0.34(22)	3.65±0.24(11)
9	5.2(10)	5.1(30)	5.22±0.18(7)	---	4.38±0.53(22)	4.52±0.55(14)
10	4.7(4)	4.6(5)	4.37±0.06(2)	---	4.01±0.48(20)	4.17±0.40(17)
11	4.8(2)	4.5(3)	4.30±0.14(3)	---	3.97±0.50(14)	3.81±0.20(4)
12	4.6(10)	4.9(11)	4.38±0.26(3)	---	4.21±0.60(21)	3.44±0.08(2)
13	5.8(20)	5.4(36)	5.09±0.16(5)	---	5.29±0.26(30)	5.47±0.43(16)
14	4.7(4)	4.6(4)	5.06(1)	---	3.49±0.47(11)	3.92±0.23(6)
15	5.1(10)	5.0(21)	5.01±0.52(10)	4.7(2)	4.62±0.41(26)	4.44±0.42(11)
16	5.2(9)	5.0(23)	4.89±0.22(5)	4.8(1)	4.43±0.25(23)	4.34±0.30(18)
17	5.0(8)	5.0(15)	4.64±0.41(6)	5.1(1)	4.69±0.29(26)	4.42±0.36(9)
18	4.9(7)	4.6(6)	4.56±0.31(5)	---	4.07±0.39(20)	4.03±0.43(3)
19	5.2(18)	5.0(30)	4.89±0.29(11)	---	3.48±0.42(3)	---
20	5.7(29)	5.7(46)	5.73±0.29(11)	---	3.66±0.34(4)	---
21	5.5(14)	5.3(37)	5.09±0.29(8)	---	3.73±0.37(9)	3.02(1)
22	6.3(23)	6.3(71)	6.33±0.23(9)	4.7(1)	5.02±0.32(27)	4.64±0.24(18)
23	5.5(22)	5.5(39)	5.07±0.32(6)	5.3(3)	5.08±0.33(25)	4.90±0.28(16)
24	5.5(34)	5.5(51)	5.29±0.36(11)	4.9(1)	4.74±0.21(28)	4.66±0.40(13)
25	5.1(6)	4.9(10)	4.46±0.40(6)	---	2.76±0.57(3)	---
26	4.9(4)	4.8(6)	4.26±0.11(2)	---	3.90±0.52(7)	3.40(1)
27	5.1(2)	4.6(6)	4.53±0.32(4)	---	4.99±0.33(19)	5.13±0.19(8)
28	5.2(5)	5.2(5)	4.89(1)	---	3.77±0.18(2)	---
29	4.6(6)	4.6(6)	4.66±0.45(3)	---	3.32±0.21(3)	---
30	5.1(14)	5.0(25)	5.03±0.34(6)	---	3.96±0.27(8)	---



TABLE 2 (continued)

31 E	5.1(12)	5.0(19)	4.67+0.33(10)	---	3.65+0.32(3)	---
32	5.0(8)	5.0(14)	4.89+0.25(5)	5.5(2)	5.04+0.28(23)	5.07+0.25(11)
33	4.9(7)	5.1(17)	4.83+0.40(6)	---	4.55+0.40(20)	4.30+0.29(7)
34	5.1(3)	4.7(14)	4.36+0.26(3)	---	3.38+0.52(8)	---
35	5.1(9)	5.1(20)	5.00+0.33(5)	5.6(2)	5.06+0.28(23)	5.14+0.24(11)
36	5.1(7)	5.1(17)	4.67+0.20(8)	5.4(2)	5.00+0.28(24)	5.00+0.30(11)

a The hypocentral coordinates of each event are given in Table 1.

b The numbers in parentheses indicate the number of stations whose data were used.

c The number following the "+" sign is the standard deviation.

TABLE 3. EARTHQUAKES FOR WHICH  $m_b(\text{ISC}) - M_S \leq 1.2$

Date	Origin Time	Lat. ( $^{\circ}\text{N}$ )	Long. ( $^{\circ}\text{E}$ )	$m_b - M_S$	Location
03-09-71	18-42-16.0	28.9	103.7	1.4	Szechwan
09-09-71	06-51-08.8	38.2	20.1	1.4	Greece
04-10-71	22-21-57.2	43.1	12.9	1.2	Central Italy
24-10-71	08-59-04.6	28.2	87.2	1.9	Tibet
31-10-71	15-54-47.9	26.2	90.7	1.5	Eastern India
23-11-71	17-40-05.8	28.8	103.7	1.4	Szechwan
24-11-71	08-23-24.6	38.7	73.3	2.2	Tadzhikistan-Sinkiang
04-12-71	08-38-00.7	27.9	87.9	2.0	Nepal
20-12-71	05-05-24.0	41.1	48.2	1.4	E. Caucasus
27-12-71	20-59-34.1	35.1	73.1	1.6	Pakistan
06-01-72	09-41-33.2	30.3	50.5	1.4	Iran
25-01-72	20-24-38.9	43.8	13.4	1.3	Central Italy
25-01-72	23-22-17.1	43.8	13.4	1.6	Central Italy
04-02-72	14-08-21.7	30.3	84.6	1.2	Tibet
06-02-72	07-30-11.4	41.6	82.2	1.2	S. Sinkiang
20-02-72	03-02-14.0	34.6	80.3	1.3	Tibet
28-02-72	02-04-35.0	40.4	29.1	1.2	Turkey
03-03-72	21-26-51.3	44.7	18.4	1.5	Yugoslavia
04-03-72	08-22-16.6	42.1	83.3	1.2	S. Sinkiang
08-04-72	06-42-13.3	29.7	89.5	1.4	Tibet
09-04-72	10-43-56.3	42.0	84.6	1.5	S. Sinkiang
06-05-72	22-05-19.9	28.3	102.3	1.3	Szechwan
07-05-72	06-36-03.0	40.2	78.9	1.2	S. Sinkiang
08-05-72	09-20-54.5	41.6	23.5	1.3	Greece-Bulgaria
16-05-72	10-59-52.6	28.4	52.6	1.3	Greece-Bulgaria
20-05-72	06-44-26.1	28.3	52.8	1.2	S. Iran
23-05-72	03-14-28.2	41.7	23.6	1.7	S. Iran
23-05-72	18-17-14.1	38.5	70.2	> 1.6	Greece-Bulgaria
30-05-72	06-38-16.8	38.3	69.5	1.2	Tadzhikistan
14-06-72	00-49-54.4	40.1	51.9	1.5	Tadzhikistan
17-06-72	09-02-47.5	48.3	14.5	1.3	Caspian Sea
03-09-72	20-32-18.4	35.9	73.5	1.4	Austria
29-09-72	13-56-59.5	39.7	77.8	1.4	N.W. Kashmir
				1.3	S. Sinkiang



TABLE 4. HYPOCENTRAL COORDINATES OF FORESHOCKS,  
MAINSHOCKS AND AFTERSHOCKS STUDIED

Region	Date	Origin Time	Lat. (°N)	Long. (°E)	Depth (km)	$m_b$	$M_s$
Szechwan	16-08-71	04-58-00.3	28.9	103.7	19	5.7	4.8
	16-08-71	13-29-24.8	28.8	103.7		4.8	4.0
	16-08-71	18-53-54.7	28.9	103.6	17	5.4	5.4
	16-08-71	22-37-33.6	28.8	103.6	13	5.3	4.7
	17-08-71	09-36-15.5	28.9	103.7		5.0	4.3
	17-08-71	17-07-40.4	28.9	103.7		4.9	4.2
	03-09-71	18-42-16.0	28.9	103.7	15	4.7	3.3
	04-09-71	01-10-33.0	29.0	103.7		4.9	3.8
	04-11-71	20-12-20.5	28.8	103.7		4.9	3.9
	23-11-71	17-40-05.8	28.8	103.7		4.8	3.4
Iraq-Iran	14-01-72	22-10-03.7	32.8	46.9		5.0	4.1
	10-06-72	19-31-41.8	32.9	46.3		4.7	3.6
	12-06-72	13-34-00.7	33.1	46.3	16	5.3	4.9
	12-06-72	13-39-58.8	33.1	46.2		5.0	4.5
	13-06-72	00-55-37.3	33.1	46.3	12	5.1	4.5
	14-06-72	04-34-28.1	33.0	46.1	15	5.3	4.1
	23-06-72	08-39-35.8	32.9	46.2		4.5	3.8
	21-09-71	09-13-51.5	32.4	91.8		4.8	4.7
	24-10-71	08-59-04.6	28.2	87.2	20	4.8	2.9
	29-10-71	17-16-52.1	34.1	86.3	18	4.7	4.2
Tibet	04-12-71	08-38-00.7	27.9	87.9		4.9	3.2
	04-02-72	14-08-21.7	30.4	84.6		5.0	4.2
	20-02-72	03-02-14.0	34.6	80.3		4.8	3.5
	15-03-72	06-00-32.4	30.4	84.5		5.1	4.1
	08-04-72	06-42-13.3	29.7	89.5		4.4	3.4
	21-04-72	21-19-29.5	35.0	81.0		4.9	4.0
	28-04-72	00-52-56.8	31.3	84.9		5.2	4.2
	14-07-73	04-51-21.0	35.2	86.5	19	6.0	6.6
	14-07-73	13-39-30.0	35.3	86.6	22	6.0	5.4

TABLE 4 (Continued)

New Hebrides	23-01-72	17-18-39.4	-13.1	166.3	25	5.3	5.4
	23-01-72	18-04-00.2	-13.2	166.6		5.5	5.5
	23-01-72	21-17-52.1	-13.2	166.4	28	5.9	6.8
	24-01-72	00-18-33.5	-13.2	166.3		4.9	5.1
	24-01-72	03-55-42.5	-13.0	166.4	26	5.9	5.9
	24-01-72	09-27-07.3	-13.2	165.9		4.7	4.9
	24-01-72	15-42-51.9	-13.2	166.5		4.5	4.4
	26-01-72	01-44-45.5	-13.0	166.3		5.1	4.9



## FIGURE CAPTIONS

Figure 1.  $m_b:M_s$  values of Eurasian underground explosions. The  $m_b$  values are those of the International Seismological Centre, and the  $M_s$  values are those determined in the present study. The solid-line curves mark the upper and lower bounds of the explosion data. The dashed-line curve is the NTS explosion curve, where  $M_s$  is determined from 20-second period surface waves, as given by Evernden et al (1971).

Figure 2.  $m_b:M_s$  values of anomalous Eurasian earthquakes, for which  $m_b-M_s \geq 1.2$ . The solid-line curves are the upper and lower bounds of the explosion data, as given in Figure 1.

Figure 3.  $m_b:M_s$  values of Eurasian oceanic margin earthquakes of 1972. The solid-line curves are the upper and lower bounds of the explosion data, as given in Figure 1.

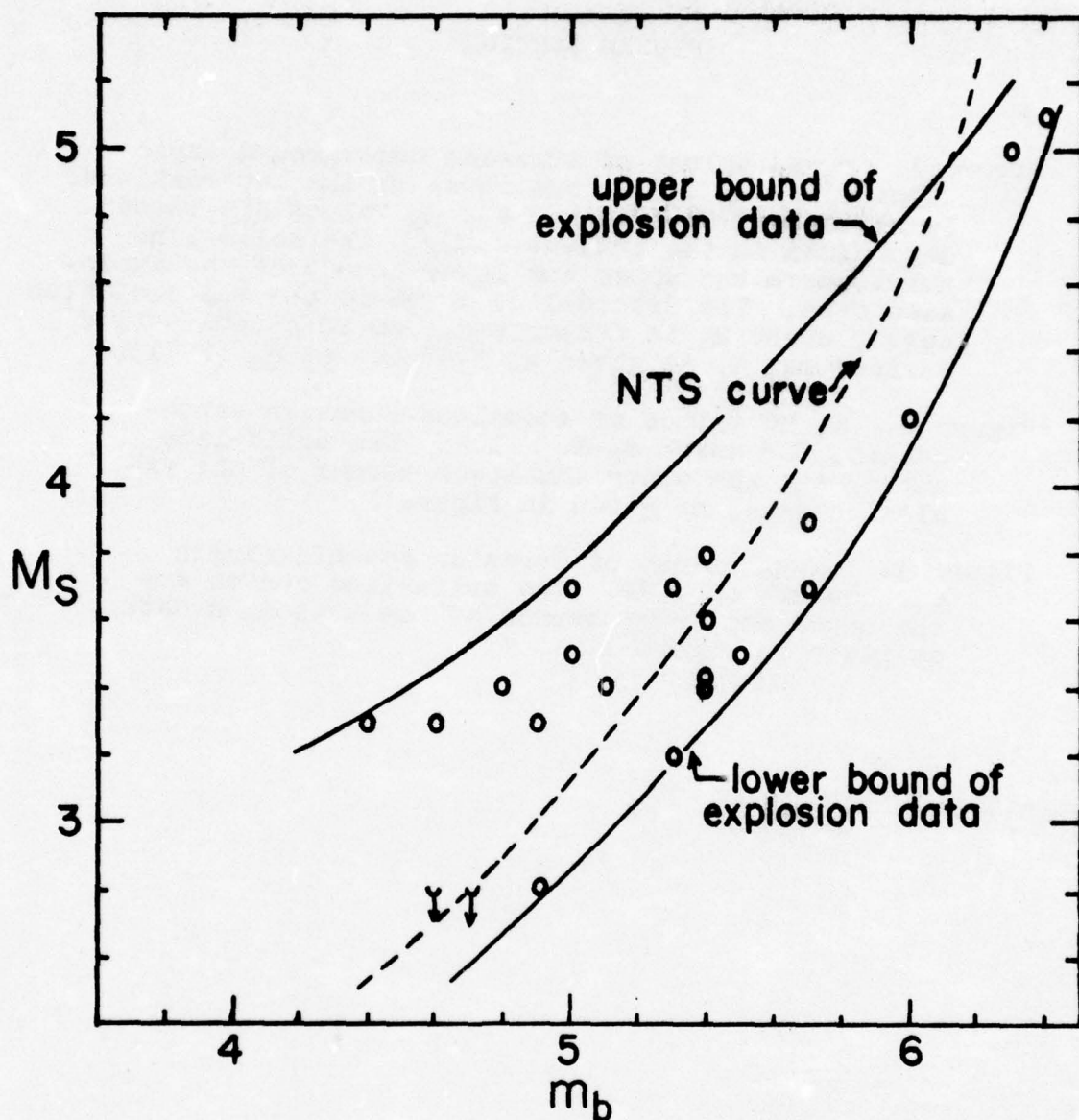


Figure 1.  $m_b:M_s$  values of Eurasian underground explosions. The  $m_b$  values are those of the International Seismological Centre, and the  $M_s$  values are those determined in the present study. The solid-line curves mark the upper and lower bounds of the explosion data. The dashed-line curve is the NTS explosion curve, where  $M_s$  is determined from 20-second period surface waves, as given by Evernden *et al* (1971).



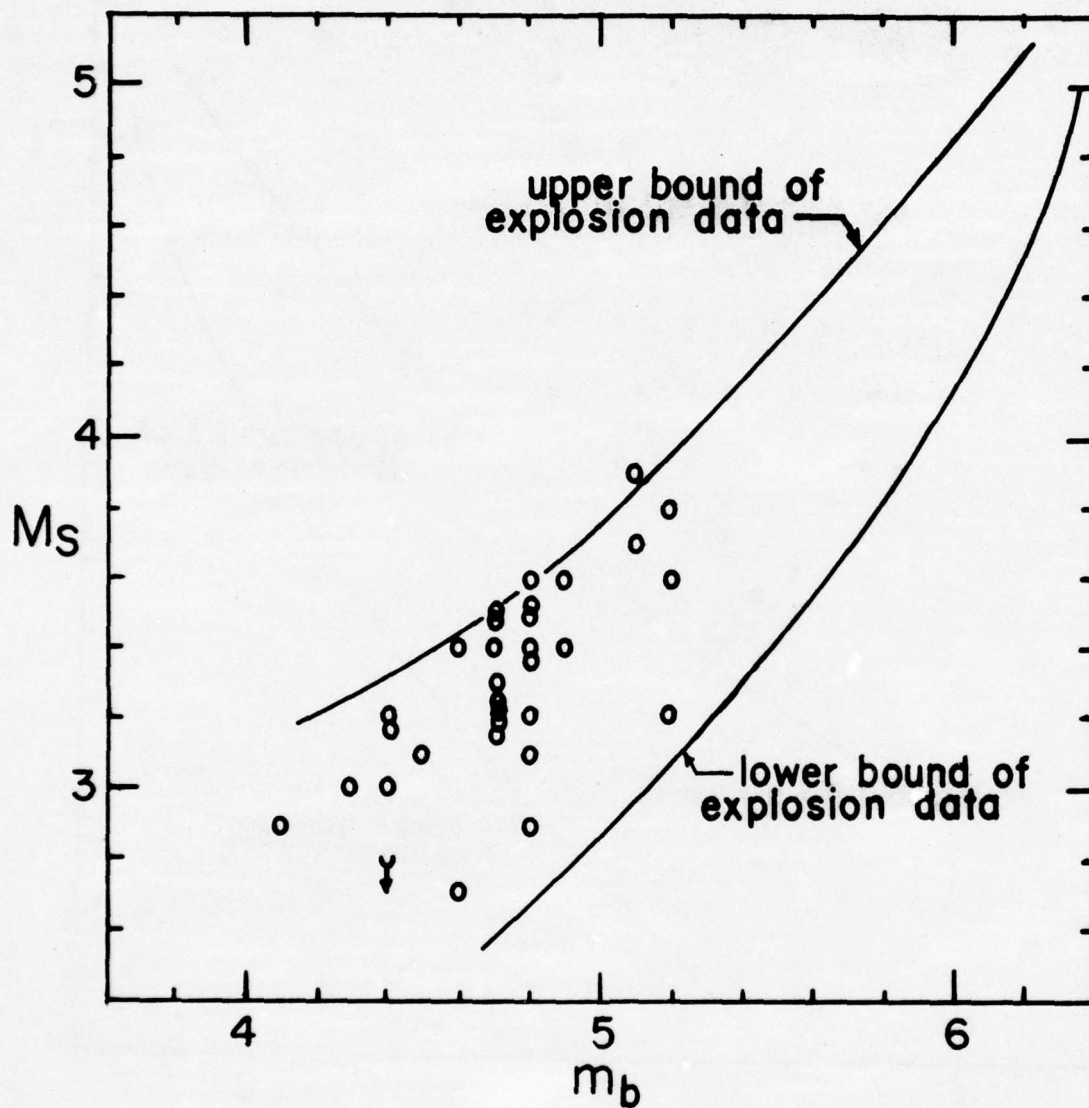


Figure 2.  $m_b:M_s$  values of anomalous Eurasian earthquakes, for which  $m_b - M_s \geq 1.2$ . The solid-line curves are the upper and lower bounds of the explosion data, as given in Figure 1.

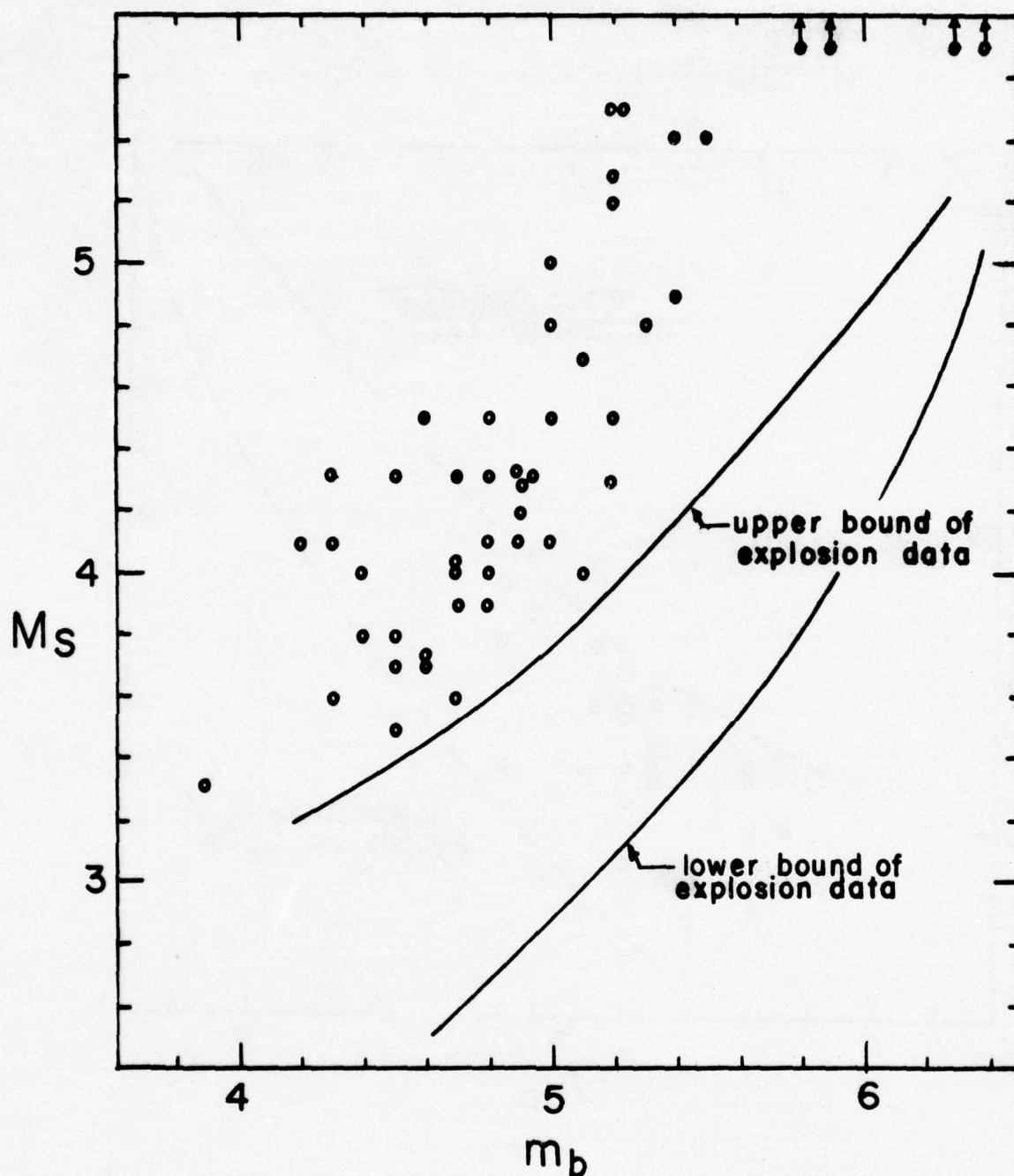


Figure 3.  $m_b:M_s$  values of Eurasian oceanic margin earthquakes of 1972. The solid-line curves are the upper and lower bounds of the explosion data, as given in Figure 1.



## APPENDIX 1.

### SPECTRAL AND MAGNITUDE CHARACTERISTICS OF ANOMALOUS EURASIAN EARTHQUAKES

by

So Gu Kim\* and Otto W. Nutt11

#### ABSTRACT

A number of mainshock-aftershock sequences in the Eurasian interior contain some aftershocks whose  $m_b:M_s$  values are close to those of underground explosions. This paper is concerned with a study of the amplitude spectra of the P waves and Rayleigh waves for earthquakes of those mainshock-aftershock sequences. It is found that for any given sequence studied there is little if any variation in focal depth or focal mechanism. This rules out variations in these quantities as being the cause of anomalous  $m_b:M_s$  values. A study of the P-wave spectra establishes that one or both of the corner periods of anomalous earthquakes are smaller than those of non-anomalous earthquakes of the same moment. Thus the cause of anomalous  $m_b:M_s$  values of the earthquakes studied is a relative enrichment of the short-period portion of the spectrum of the anomalous events, which cannot be attributed to focal depth or focal mechanism.

\* Present address: Seismograph Service Corporation, Tulsa, Oklahoma.

## INTRODUCTION

A recent study of  $m_b$  and  $M_3$  values of approximately 300 intermediate-size Eurasian shallow-focus earthquakes revealed that most anomalous earthquakes (events whose  $m_b:M_3$  values are closer to those of explosions than to those of ordinary earthquakes) occurred in the continental interior rather than at the oceanic margins (Nuttli and Kim, 1975). Additional study has established that the majority of anomalous events occurred as aftershocks, or in some cases foreshocks, of non-anomalous mainshocks. Not all foreshocks or aftershocks, however, were found to be anomalous.

The validity of using  $m_b:M_3$  values in distinguishing between earthquakes and explosions has been explained (Molnar et al, 1969; Lieberman and Pomeroy, 1970) in terms of a number of factors, namely source-time functions, source size, properties of the travel path, source mechanism and focal depth. Tsai and Aki (1971) argued against the first two factors as being the primary cause of the difference in  $m_b:M_3$  values for earthquakes and explosions. Rather they maintained that the last two are dominant after corrections due to differences in travel path are taken into account. Evernden (1975) also concluded that anomalous events can be explained principally by differences in source mechanism and focal depth.

On the other hand, Kanamori and Anderson (1975) demonstrated that inter-plate earthquakes which occur along or parallel to major plate boundaries show low stress drop compared to intra-plate earthquakes which occur within the plates. Forsyth (1975)



concluded that anomalous  $m_b:M_S$  values observed for a foreshock-mainshock-aftershock sequence in the Kirgiz-Sinkiang border region resulted from the source finiteness or the rupture-time duration rather than from the focal depth or the focal mechanism.

#### EARTHQUAKES STUDIED

In this paper we restrict our discussion to single mainshock-aftershock sequences in the Szechwan province of China, in Tibet, in the Iraq-Iran border region and in the New Hebrides Islands. Table 1 gives the latitude, longitude, origin time and focal depth as determined by the National Earthquake Information Service for the earthquakes whose focal mechanisms and P-wave and Rayleigh-wave spectra were determined in this study. Also included are the  $m_b$  and  $M_S$  values as determined by us.

An inspection of Table 1 will show that the hypocentral coordinates of the earthquakes of a given sequence show little variation. The time differences,  $pP - P$  and  $sS - S$ , when they could be observed, indicated a nearly constant focal depth for all the events of a sequence. Further evidence for the same focal depth is given by the periods of the minimum in the Rayleigh-wave spectra, which for a given station are almost constant for all the events of a sequence. Sample Rayleigh-wave spectra for two stations for the Szechwan and New Hebrides earthquakes are given in Figures 1 and 2, respectively.

For all four earthquake sequences the focal mechanisms of individual earthquakes of a given sequence are remarkably similar. This is demonstrated in Figures 3a and 3b, in which

solutions based on the sign of the onset of the long-period P motion are presented.

By selecting for study events of mainshock-aftershock sequences which have the same hypocentral coordinates, the same focal mechanism and the same transmission path, we eliminate many of the quantities which have been proposed in explanation of anomalous  $m_b:M_s$  values. We can thus restrict our attention to quantities such as source finiteness, rupture velocity and stress drop.

Although we shall not present a physical explanation as to why some earthquakes have anomalous  $m_b:M_s$  values, we wish to point out certain ways in which the spectra of anomalous earthquakes differ from those of non-anomalous ones. We shall leave to others the interpretation of these spectral differences, and merely note that differences in the corner periods and slopes of body-wave spectra have been interpreted in terms of source finiteness (Hanks and Wyss, 1972; Forsyth, 1975) and of fractional stress drop (Brune, 1970).

#### TIME-DOMAIN OBSERVATIONS

Direct observation of the seismograms led us originally to a study of mainshock-aftershock sequences in a search for anomalous events. That is, by looking at the seismograms we could see that events which produced nearly the same P-wave amplitudes at a station produced noticeably different Rayleigh-wave amplitudes. Figure 4 gives some examples. On the left-hand side are the seismograms for the Szechwan earthquakes. The upper left shows the P-wave motion at two stations, EUL



and SHK, for the three events. Maximum amplitudes in the first few cycles are about the same (the onset of the P motion at SHK for event no. 3 is obscured by the minute marks; its peak and trough almost touch the trace above and below, respectively). The Rayleigh-wave amplitudes for event no. 3, as recorded at station SHI, are noticeably less than for events 1 and 2.

The P waves and Rayleigh waves for the two Tibetan events are given in the right-hand side of Figure 4. The P-waves are shown for stations NUR, STU and KTG and the Rayleigh waves for station KTG. Although the duration of the P waves of event no. 1 is greater than of no. 2, the amplitudes of the first few cycles of P of no. 1 are almost the same as the amplitude of no. 2, which would result in nearly similar  $m_b$  values for the two earthquakes. The surface-wave amplitudes of event no. 1, however, are much greater than of event no. 2, as can be seen from the lower right-hand figure.

Figures 5 and 6 show as examples  $m_b:M_s$  plots for the Tibet and New Hebrides earthquakes, respectively. The points labeled 1 and 2 in Figure 5 refer to the Tibetan earthquakes no. 1 and 2 in Table 1. The other points refer to earthquakes for which  $m_b:M_s$  values could be determined but which were too small for spectral analysis. Curve a in Figure 5 is a least-square linear fit to  $m_b:M_s$  data from 64 non-anomalous Eurasian earthquake values, and curve c a similar fit for 11 Eurasian underground explosion values. The data sets were taken from Nuttli and Kim (1975). Curve b is a linear fit to the Tibetan data points, indicated by x's in the figure. Note that the mainshock (event no. 1) as well as two of the other Tibetan events would be

considered non-anomalous. Event no. 2, as well as 6 others, would be considered suspicious by the  $m_b:M_S$  criterion. The two remaining events definitely fall in the explosion population.

Curves a and c of Figure 6 are the same as described for Figure 5. If event no. 2 is considered to be the mainshock, its  $M_S$  value is even larger than for the ordinary Eurasian earthquake of  $m_b = 5.9$ . The foreshock (no. 1) and all the aftershocks also scatter around curve a. Curve b is the linear fit to the eight data points of the figure. Thus none of the New Hebrides earthquakes would be considered to have anomalous  $m_b:M_S$  values.

#### RAYLEIGH-WAVE SPECTRA

Rayleigh-wave ground-motion spectra were obtained from analysis of the long-period, vertical-component seismograms. Stations were selected so that the path from epicenter to station was pure continental or pure oceanic. The observed spectra were adjusted for the effects of geometric spreading and anelastic attenuation, to reduce them as if the seismograph station were 1000 km from the epicenter.

Sample spectra are shown in Figures 1 and 2. Values below 10 sec are unreliable due to both small instrument magnification and low signal amplitude. The spectra can be used for two purposes: 1) to determine whether differences in log spectral amplitude at 20-sec period are equal to differences in  $M_S$  values, i.e. to test the equivalence of amplitude differences in the frequency domain with amplitude differences in the time domain, 2) to determine the seismic moment of the various earthquakes,



by comparing spectral levels of actual earthquakes with those calculated for a unit-moment, double-couple source at the appropriate azimuth for a distance of 1000 km.

Table 2 presents the  $M_S$  differences and the differences in the log spectral amplitude at 20-sec period for the 11 events in the 4 geographic regions. The number  $n$  refers to the number of stations whose spectral amplitudes were used to obtain an average  $\log_{10} \Delta A$ . In general the differences between  $\Delta M_S$  and  $\log_{10} \Delta A$  are small, of the order of 0.1 to 0.2  $M_S$  units. The exception is the set of Szechwan earthquakes; either  $M_S$  of event no. 1 is too small or its 20-sec period spectral amplitude is too large. From studies of the P-wave spectra we believe that the  $M_S$  value of this event is about 0.3 units too large, which corresponds to one standard deviation.

Table 3 compares the seismic moment, as obtained from the Rayleigh-wave spectrum, with the body-wave magnitude. From the table it can be seen that non-anomalous earthquakes of a given body-wave magnitude have larger moments than anomalous earthquakes of the same magnitude, sometimes by more than a power of ten.

#### P-WAVE SPECTRA

P-wave ground-motion spectra were determined from the LPZ and SPZ seismograms for stations at teleseismic distances. As they were not normalized to any particular epicentral distance, in comparing them one should compare the spectra of an individual station for an individual mainshock-aftershock sequence. Figures 8, 9, 10 and 11 give sample spectra for a few of the stations whose data were utilized. The small open circles refer to

spectral values obtained from analysis of the short-period seismograms, and the continuous curve to spectral values obtained from the long-period seismograms. Because of low signal-to-noise ratios the spectral values obtained from the long-period seismograms are not valid for periods less than 3 sec.

The spectra can be approximated by three straight-line segments, namely: a flat portion extending from an infinite period to a corner period called  $T_{01}$ , a sloping straight line extending from the corner period  $T_{01}$  to a second corner period  $T_{12}$ , and a third straight line, of slope greater than the second, extending from corner period  $T_{12}$  to the short periods. The first and second of these curves, intersecting at period  $T_{01}$ , are superimposed on the spectra in Figures 7 through 10. From the figures it can be noted that in general the non-anomalous earthquakes have larger values of  $T_{01}$  than the anomalous ones.

Figure 11 shows simplified P-wave spectra for each of the four earthquake sequences, as determined from the seismograms of a single station for an individual sequence. In most cases the part of the spectrum between the corner periods  $T_{01}$  and  $T_{12}$  has a slope of 1.3 to 2.0, and the part between  $T_{12}$  and 1-sec period has a slope of 3 to 4. Differences in spectral level at 1-sec period are in general in good agreement with  $m_0$  differences as obtained from time-domain measurements of the seismograms. Differences in spectral level at the long periods agree in a qualitative, if not always an exact quantitative, way with differences in seismic moment and  $M_3$ .

The curves for NUR-Tibet of Figure 11 show that although the two earthquakes have the same  $m_b$  (1-sec spectral amplitude), the non-anomalous earthquake (no. 1) has longer corner periods and a larger seismic moment. The curves for TIK-Szechwan of Figure 11 also show approximately the same spectral levels at 1 sec, but lesser corner periods and long-period amplitudes for anomalous events no. 3 and 1. Similarly, anomalous Iraq-Iran events no. 2 and 3 have about the same spectral amplitudes at 1 sec, but lesser corner periods than the non-anomalous event no. 1. If we consider the seismic moment, proportional to the long-period spectral amplitude, to be a more fundamental property of earthquakes than the  $m_b$  value, then we can conclude that for a given seismic moment an anomalous earthquake has smaller corner periods and a larger 1-sec spectral amplitude than a non-anomalous one.

#### DISCUSSION AND CONCLUSIONS

We have shown that earthquakes with anomalous  $m_b:M_0$  values occur in some of the foreshocks and aftershocks of sequences in Szechwan Province, Tibet and Iraq-Iran earthquakes of the Eurasian interior. The earthquakes in a given sequence, non-anomalous and anomalous alike, have similar focal depth and focal mechanism. Thus neither differences in these focal parameters nor in the transmission path from source to station can be called upon to explain the anomalous earthquakes.

In all, we considered 29 earthquakes in the regions mentioned above plus 8 in the New Hebrides region. Although there



is some ambiguity as to what constitutes an anomalous  $m_b:M_s$  value, as many as 24 of the 29 can be considered to be anomalous or near-anomalous events. All of the 8 New Hebrides events, on the other hand, are non-anomalous.

We found that a common feature of the anomalous events was that the corner periods of their P-wave spectra were less than those of non-anomalous events which had the same  $m_b$  value. We also observed in the time domain, that for earthquakes of the same  $m_b$ , the duration of the short-period P-wave motion was less (more pulse-like) for the anomalous than for the non-anomalous events.

The findings of this study have some bearing on the problem of nuclear test detection, in addition to the obvious one that some intra-plate foreshocks and aftershocks possess anomalous  $m_b:M_s$  values. Because these anomalous values can be explained in terms of shorter corner periods and thus an enrichment of the short-period portion of the P-wave spectrum, rather than in differences in the long-period portion or the seismic moment, it follows that methods of discrimination that compare the long-period portions of explosion and earthquake-generated waves, such as relative excitation of Rayleigh and Love waves, will be unaffected by the results discussed here. Thus the methods of discrimination which utilize exclusively the long-period portion of the surface and/or body-wave spectra should be useful in discriminating between explosions and those relatively few earthquakes which are classified as anomalous by the conventional  $m_b:M_s$  analysis.

#### **ACKNOWLEDGMENTS**

We thank Dr. Robert B. Herrmann for his critical reading of the manuscript and comments. We also wish to thank Dr. V. N. Vadkovsky, Chief of the Solid Earth Group, WDC-2, Moscow for sending us copies of U.S.S.R. seismograms.

This research was supported by the Defense Advance Research Projects Agency (Contract F 19628-73-C-0269) under the technical cognizance of Air Force Cambridge Research Laboratories.

**DEPARTMENT OF EARTH AND  
ATMOSPHERIC SCIENCES  
SAINT LOUIS UNIVERSITY**

**Manuscript received**

## REFERENCES

- Brune, J. N (1970), Tectonic stress and the spectra of seismic shear waves from earthquakes, J. Geophys. Res. 75, 4999-5009.
- Evernden, J. F. (1975), Further studies on seismic discrimination, Bull. Seism. Soc. Am. 65, 359-391.
- Forsyth, D. (1975), Causes of  $M_S:m_b$  variation within a central-Asian earthquake sequence (Abstract), Trans. Am. Geophys. Un. 56, 1024.
- Hanks, T. C. and M. Wyss (1972), The use of body-wave spectrum in the determination of seismic-source parameters, Bull. Seism. Soc. Am. 63, 561-589.
- Kanamori, H. and D. L. Anderson (1975), Theoretical basis of some empirical relations in seismology, Bull. Seism. Soc. Am. 65, 1073-1095.
- Liebermann, R. C and P. W. Pomeroy (1970), Source dimensions of small earthquakes as determined from the size of the aftershock zone. Bull. Seism. Soc. Am. 60, 879-890.
- Molnar, P., J. Savino, L. R. Sykes, R. C. Liebermann, G. Made, and P. W. Pomeroy (1969), Small earthquakes and explosions in Western North America recorded by high gain, long period seismographs, Nature 224, 1268-1273.
- Nuttli, O. W. and S. G. Kim (1975), Surface-wave magnitudes of Eurasian earthquakes and explosions, Bull. Seism. Soc. Am. 65, 693-709.
- Tsai, Y. B and K. Aki (1971). Amplitude spectra of surface waves from small earthquakes and underground nuclear explosions, J. Geophys. Res. 76, 3940-3952.



TABLE 1

## HYPOCENTRAL COORDINATES AND MAGNITUDES OF EARTHQUAKES STUDIED

Region	No.	Date	Origin Time (GMT)	Lat. (°N)	Long. (°E)	Depth (km)	$m_b$	$M_S$
Szechwan	1	16 Aug 71	04-58-00.3	28.9	103.7	19	5.7	4.8
	2	16 Aug 71	18-53-54.7	28.9	103.6	17	5.4	5.4
	3	16 Aug 71	22-37-33.6	28.8	103.6	13	5.3	4.7
Iraq-Iran	1	12 Jun 72	13-34-00.7	33.1	46.3	16	5.3	4.9
	2	13 Jun 72	00-55-37.3	33.1	46.3	12	5.1	4.5
	3	14 Jun 72	04-34-28.1	33.0	46.1	15	5.3	4.1
Tibet	1	14 Jul 73	04-51-21.0	35.2	86.5	19	6.0	6.6
	2	14 Jul 73	13-39-30.0	35.3	86.6	22	6.0	5.4
New Hebrides	1	23 Jan 72	17-18-39.4	-13.1	166.3	25	5.3	5.4
	2	23 Jan 72	21-17-52.1	-13.2	166.4	28	5.9	6.8
	3	24 Jan 72	03-55-42.5	-13.0	166.4	26	5.9	5.9

TABLE 2  
COMPARISON OF  $\Delta M_S$  AND LOG  $\Delta A$  VALUES

Region	Earthquake Pair	$\Delta M_S$	log $\Delta A$
Szechwan Province	No. 2 - No. 1	0.6	0.21 (n = 6)
	No. 1 - No. 3	0.1	0.49 (n = 6)
	No. 2 - No. 3	0.7	0.70 (n = 6)
Iraq-Iran Border	No. 1 - No. 2	0.5	0.51 (n = 4)
	No. 1 - No. 3	0.8	0.80 (n = 4)
	No. 2 - No. 3	0.4	0.29 (n = 4)
Tibet	No. 1 - No. 2	1.20	1.45 (n = 2)
New Hebrides Islands	No. 2 - No. 1	1.39	1.26 (n = 4)
	No. 3 - No. 1	0.53	0.37 (n = 4)
	No. 2 - No. 3	0.86	0.99 (n = 4)

TABLE 3  
COMPARISON OF  $m_b$  AND  $M_0$  FOR ANOMALOUS AND NON-  
ANOMALOUS EARTHQUAKES

Earthquake	$m_b$	$M_0$ (dyne-cm)	
		Anomalous	Non-anomalous
Iraq-Iran No. 2	5.1	$5.5 \times 10^{23}$	
Iraq-Iran No. 1	5.3		$1.9 \times 10^{24}$
Iraq-Iran No. 3	5.3	$2.8 \times 10^{23}$	
Szechwan No. 3	5.3	$3.2 \times 10^{23}$	
New Hebrides No. 1	5.3		$3.6 \times 10^{24}$
Szechwan No. 2	5.4		$1.8 \times 10^{24}$
Szechwan No. 1	5.7	$1.1 \times 10^{24}$	
New Hebrides No. 3	5.9		$8.5 \times 10^{24}$
New Hebrides No. 2	5.9		$9.0 \times 10^{25}$
Tibet No. 1	6.0		$3.3 \times 10^{25}$
Tibet No. 2	6.0	$1.2 \times 10^{24}$	



### Figure Captions

- Fig. 1 Rayleigh-wave spectra of Szechwan earthquakes as recorded at stations NDI and QUE and normalized to a distance of 1000 km.
- Fig. 2 Rayleigh-wave spectra of New Hebrides earthquakes as recorded at stations JCT and OGD and normalized to a distance of 1000 km.
- Fig. 3b Focal mechanism solutions for Szechwan earthquakes (above) and Iraq-Iran earthquakes (below). Compressions are indicated by octagons, dilatations by triangles and small amplitude arrivals by X's.
- Fig. 3b Focal mechanism solutions for the Tibet earthquakes (above) and the New Hebrides earthquakes (below).
- Fig. 4 (above) P-wave motion on SPZ records for the Szechwan earthquakes (left) and the Tibet earthquakes (right). For the Szechwan earthquakes the station on the left is BUL, at an epicentral distance of  $87.3^{\circ}$  and an azimuth of  $19.9^{\circ}$ , and the station on the right is SHK, at an epicentral distance of  $25.9^{\circ}$  and an azimuth of  $265.2^{\circ}$ . For the Tibet earthquakes the station on the top is NUR ( $\Delta = 40.4^{\circ}$ ,  $BAZ = 94.1^{\circ}$ ), in the middle is STU ( $\Delta = 50.7^{\circ}$ ,  $BAZ = 73.9^{\circ}$ ) and on the bottom is KTG ( $\Delta = 63.1^{\circ}$ ,  $BAZ = 0.0^{\circ}$ ).
- (bottom) Rayleigh-wave motion at station SHI ( $\Delta = 44.3^{\circ}$ ,  $BAZ = 77.8^{\circ}$ ) for the Szechwan earthquake (left) and at station KTG ( $\Delta = 63.1^{\circ}$ ,  $BAZ = 60.6^{\circ}$ ) for the Tibet earthquake (right).

- Fig. 5  $m_b:M_s$  diagram for the Tibetan earthquakes. Nos. 1 and 2 refer to the earthquakes listed in Table 1. Curve a is the linear least-square fit to 64 non-anomalous Eurasian earthquakes. Curve b is the least-square fit to the Tibetan earthquake data, indicated by X's. Curve c is the least-square fit to 11 underground Eurasian explosion data.
- Fig. 6  $m_b:M_s$  diagram for the New Hebrides earthquakes, indicated by X's. Nos. 1, 2 and 3 refer to the earthquakes listed in Table 1. Curve b is the linear least-square fit to the New Hebrides data. Curves a and c are as in Fig. 5.
- Fig. 7 P-wave amplitude spectra at stations TIK and COL for the Szechwan earthquakes. The continuous curve represents the spectrum obtained from the long-period, vertical-component seismogram and the circles the spectral values obtained from the short-period, vertical-component seismogram.
- Fig. 8 P-wave amplitude spectra at stations STU, NUR and KTG for the Tibetan earthquakes.
- Fig. 9 P-wave amplitude spectra at stations AAE and SHL for the Iraq-Iran earthquakes.
- Fig. 10 P-wave amplitude spectra at stations MAT and SHL for the New Hebrides earthquakes.
- Fig. 11 Simplified P-wave spectra for the Szechwan earthquakes as recorded at station TIK (upper left), the Iraq-Iran earthquakes as recorded at station SHL (upper right),

the Tibet earthquakes as recorded at station NUR (lower left) and the New Hebrides earthquakes as recorded at station SHL (lower right). The differences in amplitude at 1-sec period scale as differences in  $m_b$ , and the differences in amplitude at 20-sec period as differences in  $M_s$ . The corner period  $T_{12}$  for Szechwan earthquakes no. 1 and 3 is less than 1 sec.



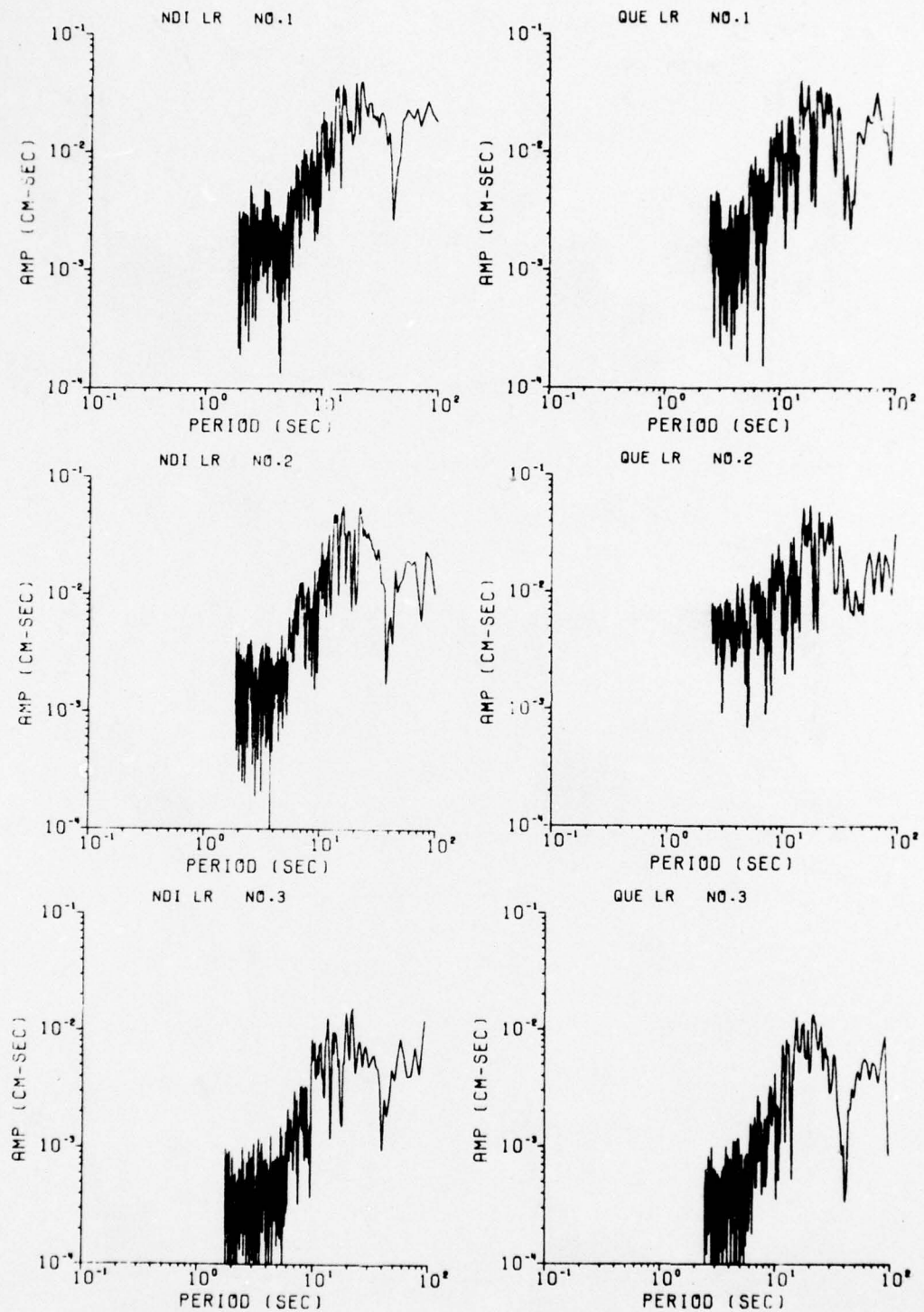


Figure 1.

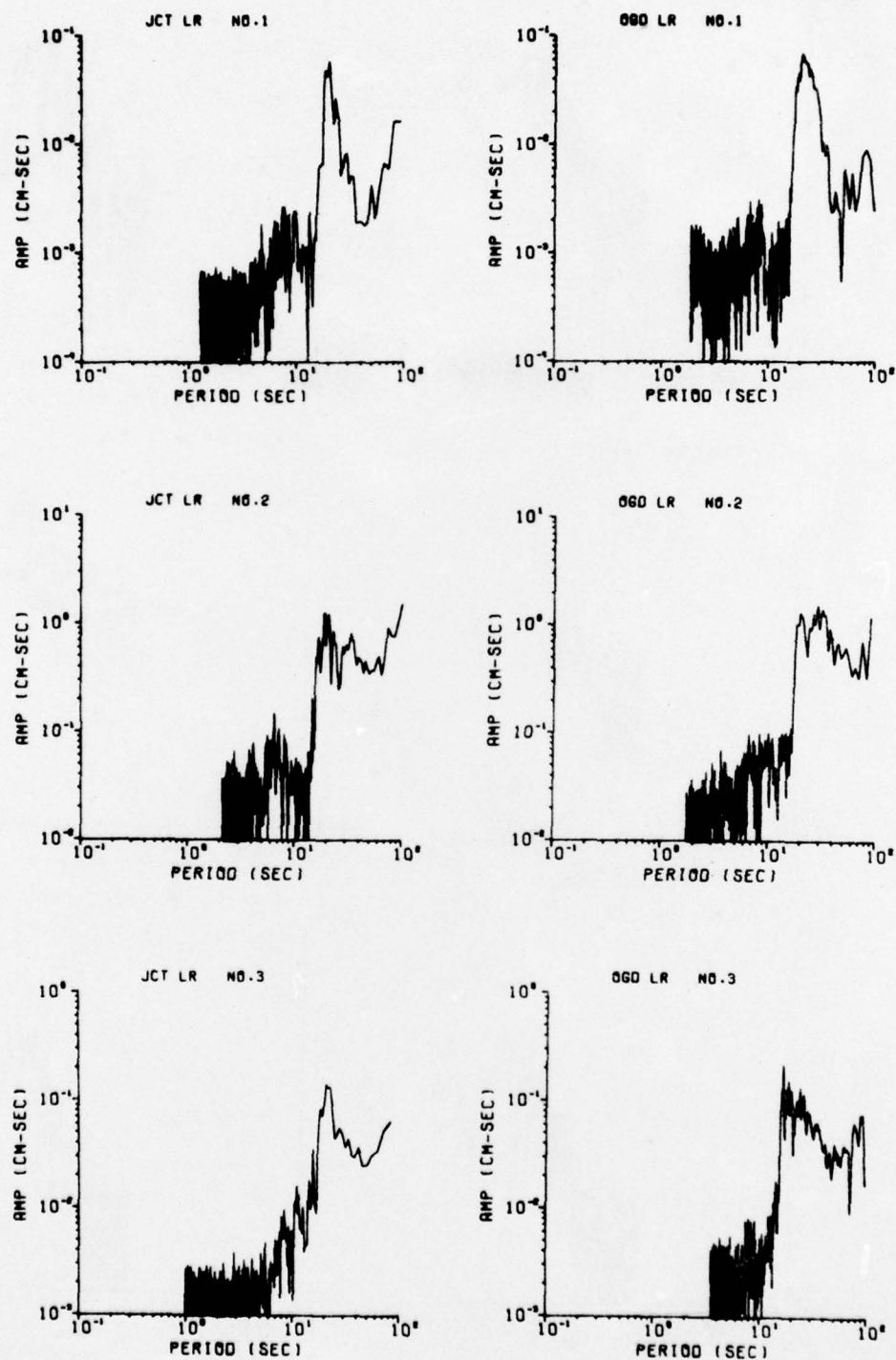


Figure 2.

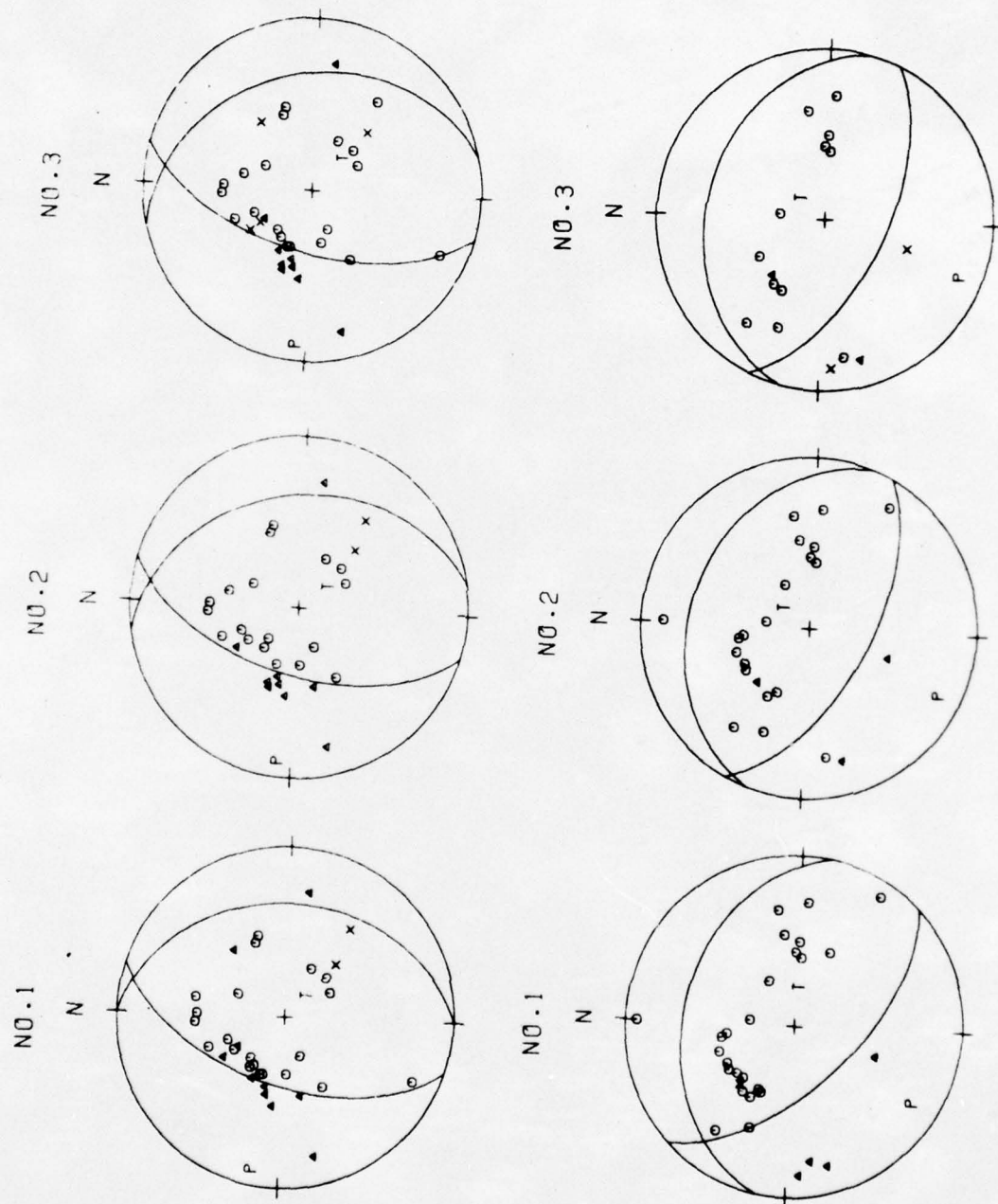


Figure 3a.



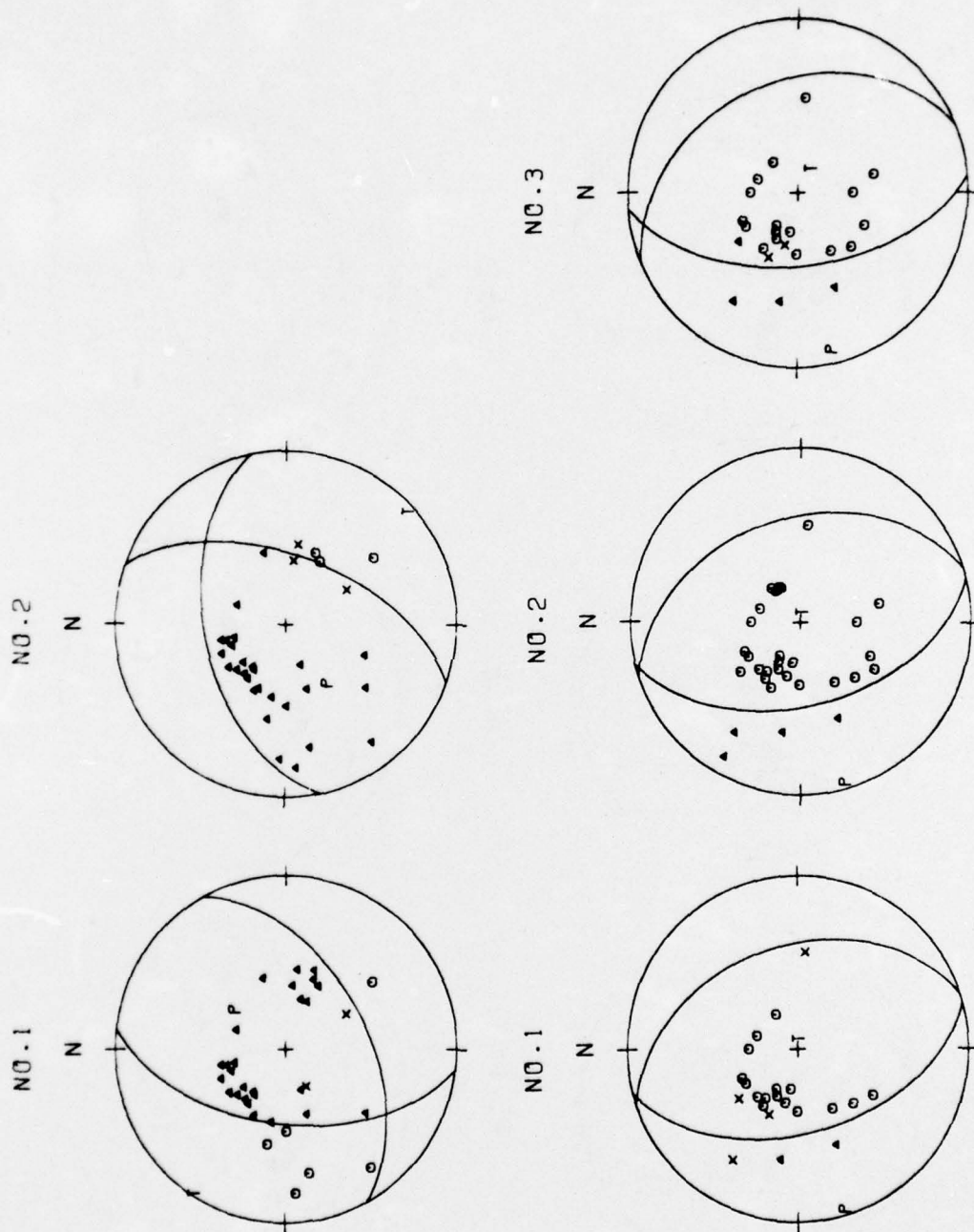


Figure 3b.



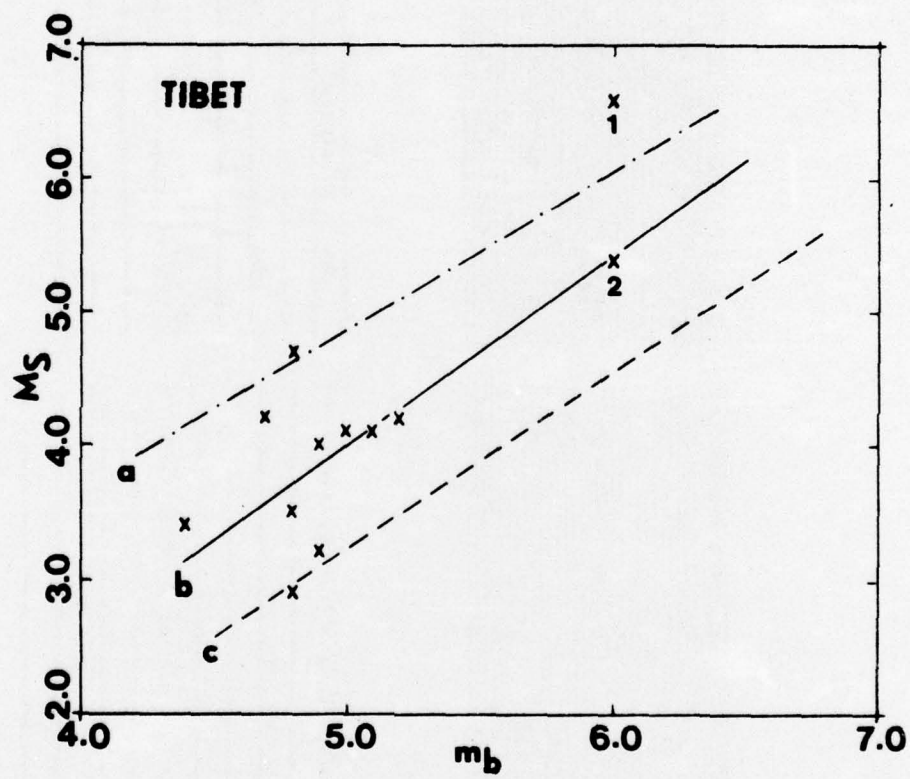


Figure 5.



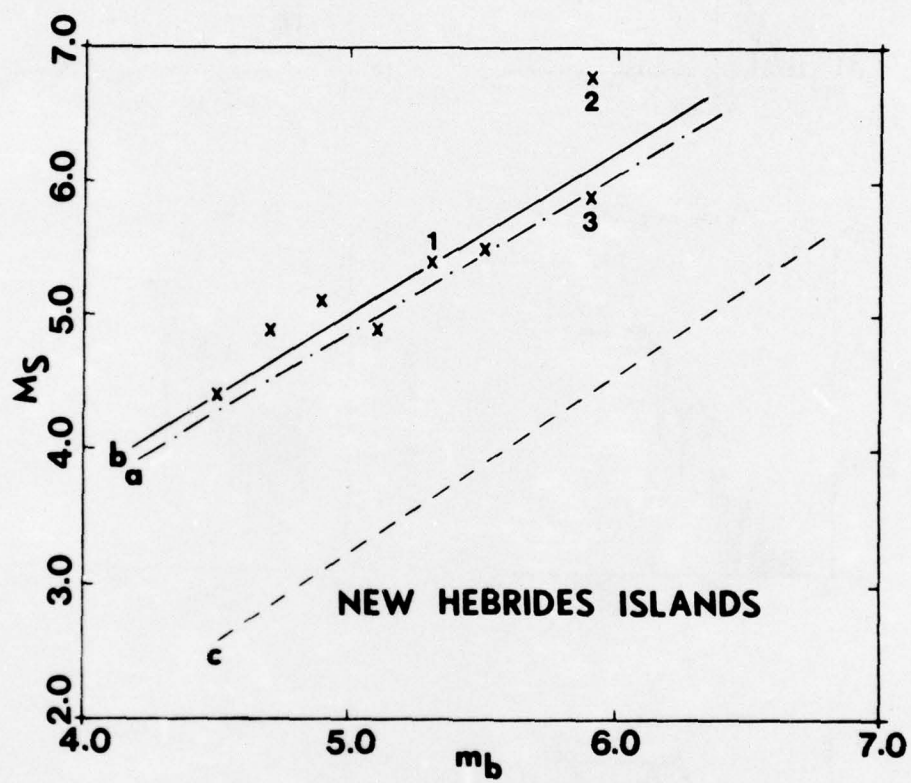


Figure 6.

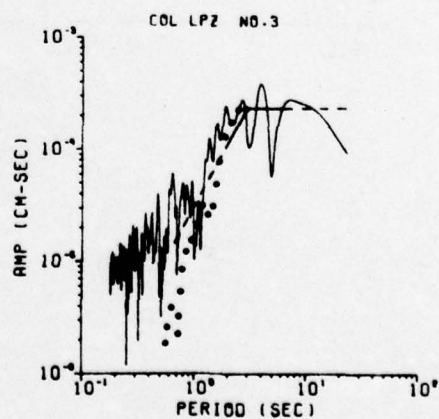
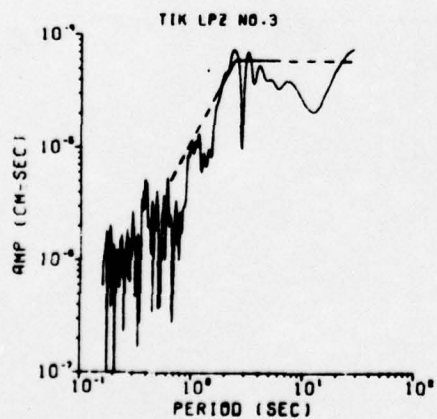
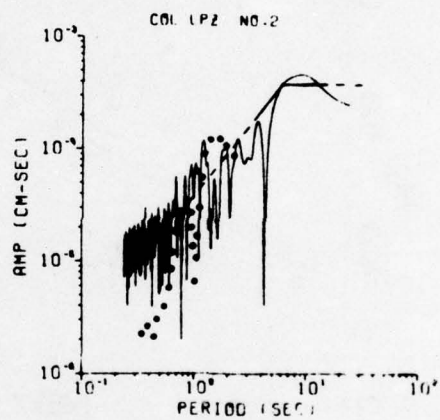
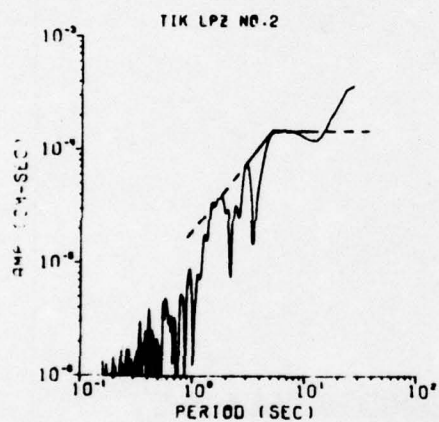
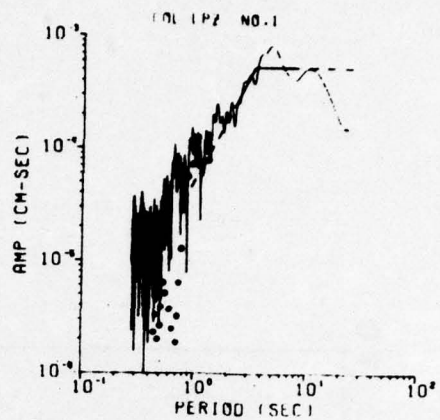
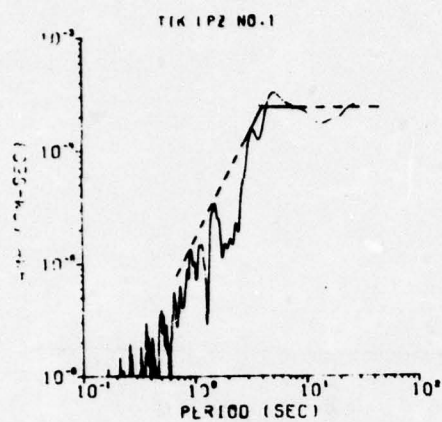


Figure 7.

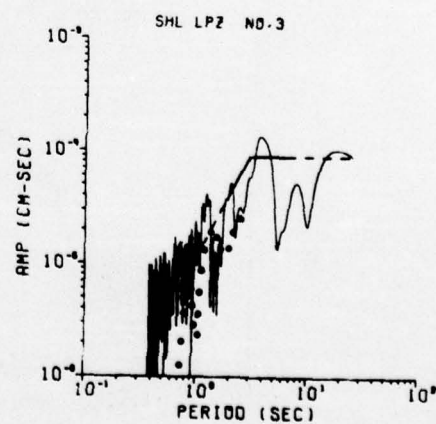
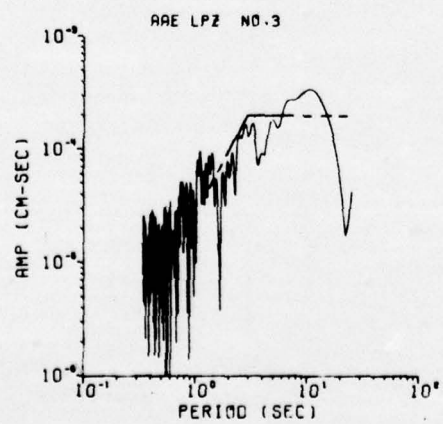
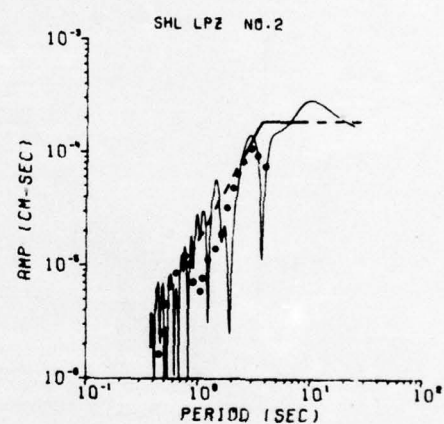
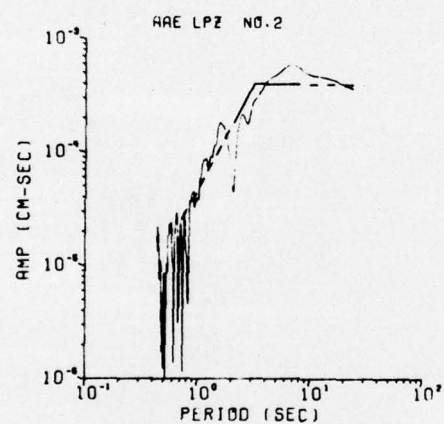
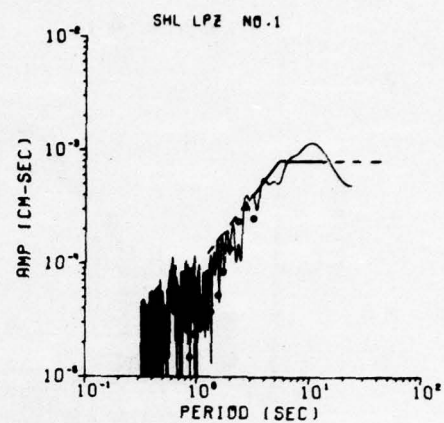
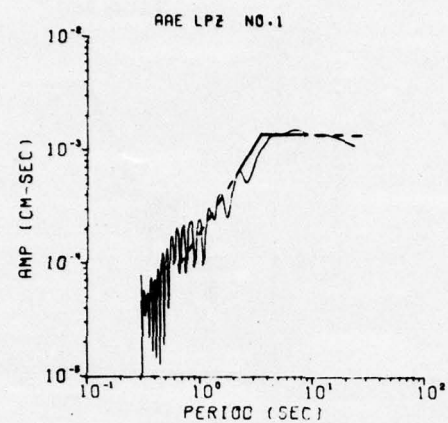


Figure 8.



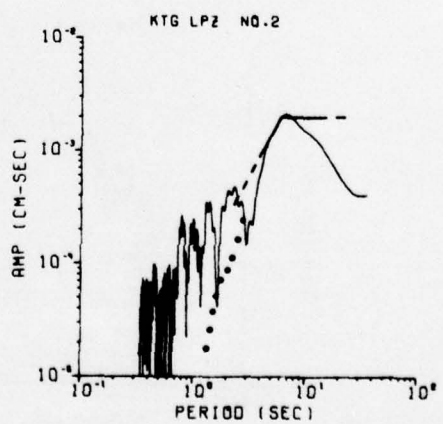
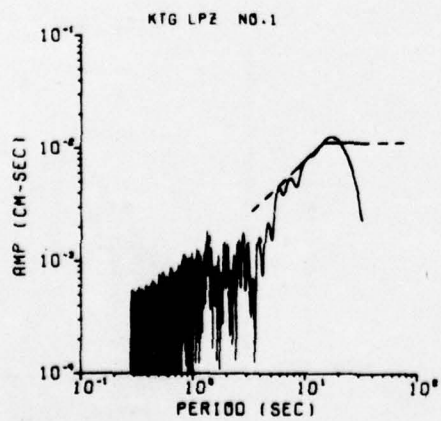
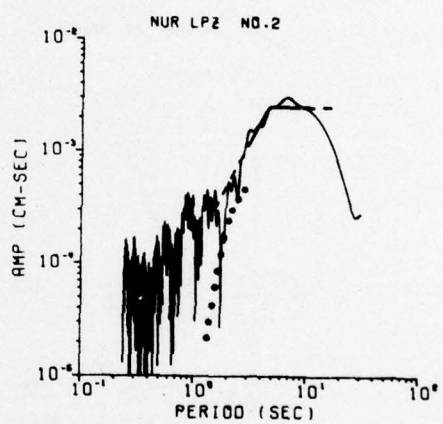
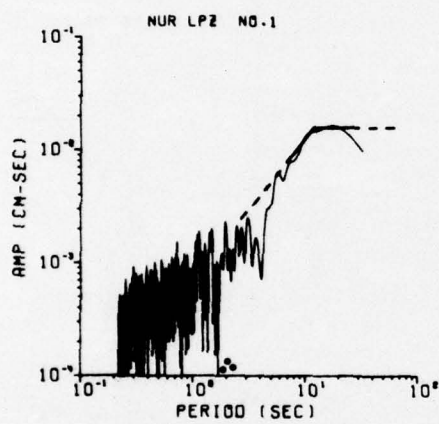
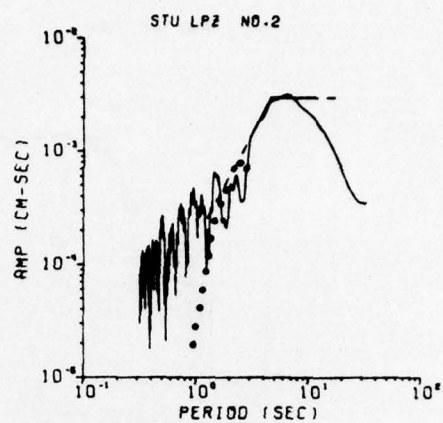
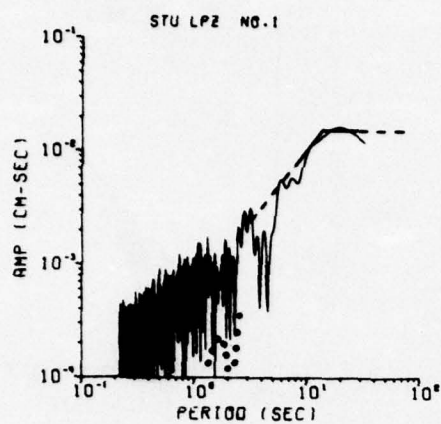


Figure 9.

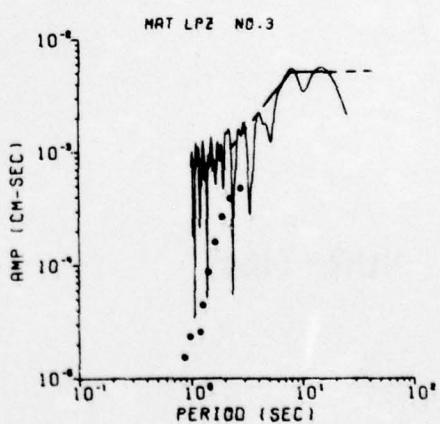
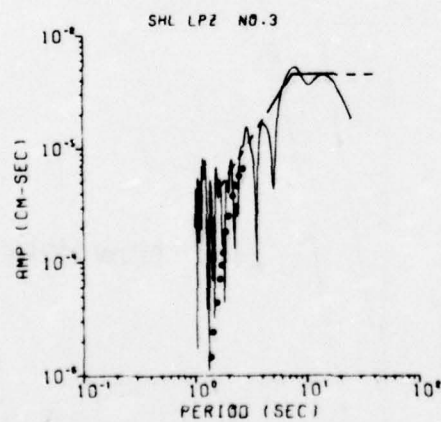
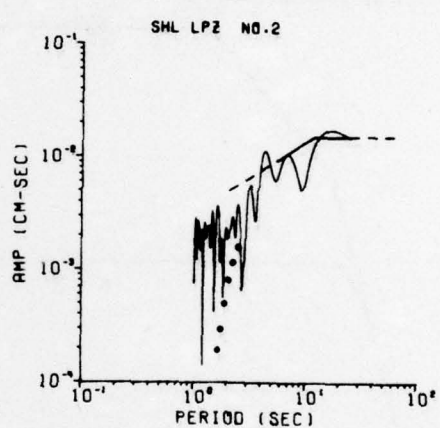
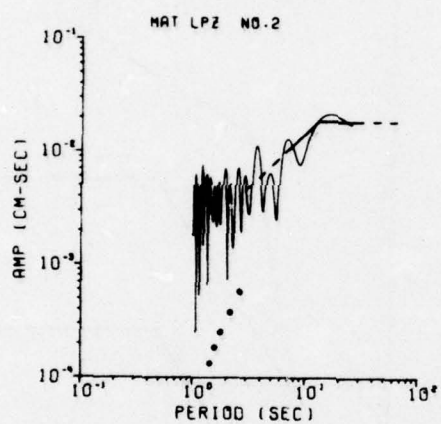
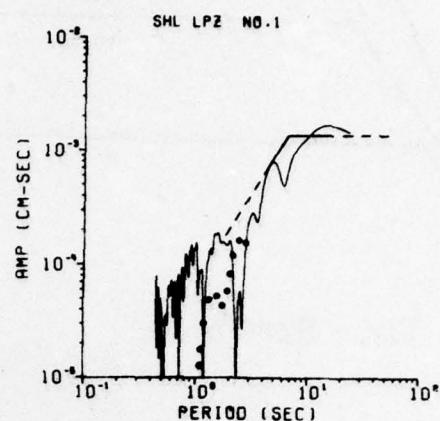
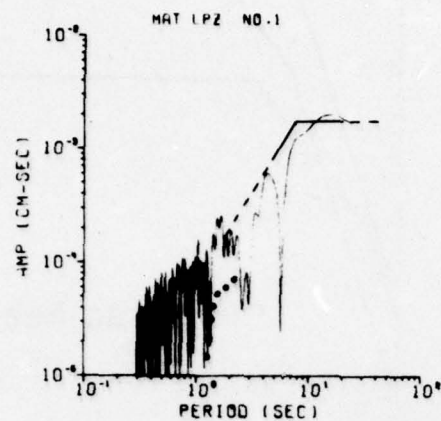


Figure 10.

